SCA-9836

APPLICATION OF CORE-LOG CORRELATION AND ARTIFICIAL NEURAL NETWORKS TO BETTER DEFINE PERMEABILITY, POROSITY AND LITHOLOGY

Stan Patniyot and Pedro A. Romero
(PDVSA – INTEVEP)

Abstract

Determining petrophysical parameters such as permeability, porosity and lithology from logs often requires the use of either empirical relationships or some form of multiple non-linear regression, because of the non-linear nature of the variables involved. A major problem of the non-linear method lies in the difficulty in choosing an appropriate mathematical model and matching the sensitivity of the model to the input variables.

Recent application of Artificial Neural Network (ANN) techniques, which use detailed core-log integration, have allowed these difficulties to be overcome. In this paper the use of a Backpropagation ANN model to provide petrophysical solutions, validated by detailed core analysis, will be demonstrated in several case studies.

Permeability determination presents a major problem because of the non-linear nature and interdependence of the reservoir variables, which constitute it. ANN's that are trained using core data are better suited to non-linear applications and yield better permeability results.

For lithofacies identification ANN techniques are faster than multivariate log-based methods because they can handle large amounts of data more efficiently.

Several case studies taken from Venezuelan reservoirs are considered. Neural network permeability and porosity transforms are developed and compared to transforms generated by conventional log-core correlation. Lithofacies are identified and are used to predict permeability corresponding to each facies. Each case study makes extensive use of core-log integration.

Introduction

The study area is located in Maracaibo Lake, in the southern part of Bloque VII. The reservoir is highly laminated with numerous shale intercalations. The stratigraphical column and lithofacies change from well to well indicating the presence of high areal and vertical heterogeneity in the reservoir.
The reservoir contains consolidated sands of the Misoa Formation, classified as C1, C2,

C3 and C4. This work is focused at the C2 and C3 sub-units, with porosity ranges of 11 to 18%, and permeability ranges of 20mD to 500mD .

Despite the wide range of **porosity**, computation using density log and core measurements yield sufficiently confident results. The results obtained by ANN can be supported with the results obtained using core-log correlation.

Permeability determination has a major uncertainty because of its inherent non-linear dependence on petrophysical quantities such as porosity, irreducible water saturation, shale volume, tortuosity, pore connectivity and other effects due to well condition or formation damage. For that reason, it is very difficult to achieve a very good core-log transform for permeability determination using standard regression methods. **Lithofacies**, on the other hand, are extremely important in identifying pay zones and also high sanding potential. Moreover, lithofacies can assist in the determination of zoned permeability and porosity relationships.

Objectives

The main objective of this work is to develop a more precise method of core permeability extrapolation using well logs as the main component of extrapolation. Other objectives are porosity and lithofacies extrapolation. The computation technique used is based on **Artificial Neural Networks**, employing an error backpropagation algorithm.

Methodology

The genetic method of reservoir characterization divides the reservoir into flow units, to enable characterization of each flow unit separately. The method emphasizes the use of lithofacies and facies architecture, to predict its petrophysical properties. Recent studies, that relate the genetic approach to the prediction of petrophysical properties, have shown that the reservoir behavior is more sensitive to the facies architecture than petrophysical properties. For instance, the presence of high vertical variations in lithofacies makes it difficult to match petrophysical properties from cores and logs .

Lithofacies with distinct depositional , diagenetic and petrophysical properties were identified first. Due to practical considerations, the available log set was reduced to deep induction, gamma ray and density log.

Lithofacies Description: Reservoirs have a random arrangement of pore spaces and flow channels. For this reason, permeability-porosity transforms are determined, generally, by statistical methods. But in the reservoir a single lithofacies may have its own permeability-porosity transforms. Every reservoir has several lithofacies that differ by the grain size, grain distribution, shale mineral type and cement type and distribution. So, a high degree of dispersion in permeability-porosity transforms is noted in most reservoirs due the variation and combination of these variables. A high dispersion in porosity and permeability can be considered an indication of the presence of reservoir heterogeneity. A simple permeability-porosity relationship, which is very often applied to the whole reservoir, will not necessarily reflect the actual reservoir heterogeneity.

The table shown in the continuation lists the predominant lithofacies in the reservoir under evaluation**.**

Table 1. Facies Description

Facies	Description
S	Sandst. cream color, coarse grained, moderately sorted. occasional conglomeritic laminations.
S3	Sandst. Cream color, medium size grain, moderately well sorted, composed of 95% quartz, feldspathic rock fragments and 2% clay. Planar cross-bedding.
S1	Sandst. Grey color, fine to medium grained, well sorted, laminated, frequent shale laminations ,composed of 90% quartz, 5% clay, feldspar fragments. Occasionally contains long clay casts. Shale laminations are horizontal and parallel.
S31	Sandst. Similar in texture and composition to facies S3, contains identical Sedimentary structures to S1.
S11	Sandst. Similar in characteristics to S3, but fewer shale laminations.
S2	Sandst. Grey color, fine grained, moderately sorted, occasionally bioturbated. Composed of 80 to 90 % quartz, 10to 15% clay, feldspar fragments.

Figs. 1A and 1B show photographs of several typical facies described in Table 1.

Neural Network Computation Description: Artificial Neural Network (ANN) are a highly parallel information processing system that are non-logarithmic and no-linear. Artificial Neural Networks are physical cell systems that can acquire, store and use experimental knowledge. The latest ANN technology has wide application in formation evaluation as correlations between well log and core data can be established, without using linear regression transforms that may be inadequate because of the inherent non-linear nature of the relationships between core and log data.

The neural network consists of layers of interconnected processors called **neurons**. Figure 2 shows the relation between entry layers, hidden layers and output layers. The number of nodes used in the entry, hidden and output layers can vary depending on the application. In the example shown in this text, five nodes were chosen for the hidden layer and produced the best correlation of data. The algorithm demonstrated in Fig 2 is the feed forward back propagation type, FFBP. This algorithm is based on the fact that there are no recurrent links in the network that can provide a feed back, which means the output of a determined node does not transmit immediately back to the same node.

An ANN emulates the behavior of the human brain in an approximate manner, executing a learning process according to external stimulus. The formal training of an ANN is performed by supervised and non-supervised algorithms. The FFBP algorithm is an example of a supervised learning algorithm, which requires prior knowledge of the required output.

Interaction between layers are governed by connections which are assigned different mathematical weights. The net is continually presented with pairs of input data and required output data during the training process. In this study, the input data used is the gamma ray log (GR), resistivity (Rt) and density (PHIT) to obtain the required output of porosity, permeability and lithofacies. These values are taken from core data and are used to train the network.

At the beginning of the process, weights are assigned randomly. Data in the entry layer are processed by neurons and the results are fed forward to the hidden layer. Neurons in the hidden layer perform a similar data processing and transfer results to the output layer. Data in the output layer are compared to required output data and the error is computed. The error is fed back to the net by adjusting the weight. The process is in essence an error minimization controlled by adjusting the weights. The FFBP algorithm uses the method of the steepest gradient to determine the optimal configuration of weights in order to minimize the error. Weights are repeatedly readjusted by a back propagation process until the specified tolerance of the error is obtained in the output layer . At this moment, the ANN is considered to be trained.

Results

Fig 3. Shows the logarithm of permeability plotted against porosity obtained from core measurements. For the example well shown, correlations are discriminated by facies. The plot shows linear relationships between the logarithm of permeability and porosity for lithofacies S3 and S31 and quadratic relationships for facies S2 and S11. This variable behavior in the correlation of the logarithm of permeability and porosity lend support to the application of ANN techniques as ANN´s automatically account for the diversified non-linear nature of the data.

Fig. 4 shows a log of the example well over the depth interval of 14660’ to 14940’. Gamma ray (GR), deep resistivity (Rt) and total porosity (PHIT) are shown in the first 3 tracks of the log. This curve set is used as input values for the ANN. Core porosity(PHINUC) values are shown in the third track. The KPORFLAG variable in the second track shows the values that were used in the training of the ANN. The fourth track shows porosity values from core with a porosity curve obtained by the ANN. The fifth column shows core permeability values obtained from other permeability transforms:

KCOREL1: $\log K = 13.4187\ PHIT + 0.3043$, for $GR<32$ API

KCOREL2: $\log K = 135.3\ (PHIT)^2 - 2.0163\ PHIT - 2.0956$

Track six shows core permeability values and the permeability curve obtained by using the ANN. In general, both standard regression and ANN obtained curves compare very well with core values. However, in intervals where a good match was not obtained, it is necessary to train the ANN with other additional log values so a better match can be obtained.

Fig 5. shows a relation between ANN porosity and core porosity, also plotted in track four in Fig. 4.

Fig 6. Shows a relation between the ANN permeability and core permeability, also plotted in track five in Fig. 4. The high correlation coefficient indicates that the permeability determined by the ANN (NNK) is matched very well to core permeability (KUCUSE).

Fig 7. Shows the correlation between ANN permeability logarithm versus core porosity, having a correlation coefficient of 0.9381, which is better than the empirical correlation KCORL2, which is 0.8155. The coefficient for KCOREL1 was not reported.

The facies classification results are shown in Fig. 8a, where the right most column shows the facies types as identified by the ANN. These results are in very good agreement with the description of lithofacies from core. Fig. 8b identifies the curve data in each column, which are defined as follows:

RECTAR2B = Lithofacies indicator selected by neural network

Lithofacies	Rectar2b	Color
S	1	white
S1	2	green
S11	3	yellow
S2	4	dark grey
S3	5	dark yellow
S31	6	light grey

GR	=	Gamma Ray Log
PHIT	=	Total porosity (from density log)
PHINUC	=	Core porosity
NNPHI	=	Neural network porosity
KNUCUSE	=	Core permeability
NNLK	=	Neural network permeability

NCFAC12B to NCFAC62B are the accumulated neuron values that correspond to each facies. These accumulated values are used to plot the lithofacies in one column.

Conclusions

This work is a part of an activity to develop Artificial Neural Network applications in the core-log correlation area. The synthetic porosity and permeability logs generated and lithofacies pattern classification, have shown that Artificial Neural Networks are a suitable tool for this application. The results that have been obtained in this study have shown that Artificial Neural Networks can be applied in the extrapolation of locally known petrophysical values in a particular formation. The next step will involve petrophysical characterization, including permeability and lithofacies prediction of the whole reservoir and will require training of the ANN with all the available data sets of the field. This will be the subject of a separate study.

Bibliography

Patniyot, S.; González, D., Revisión Petrofísica del área Norte del Campo Ceuta 2 Sur y Determinación de Correlaciones de Permeabilidad. Documento Técnico, Intevep, S.A.

Baldwin, J.L.; Otte, D.N.; Wheatley, C.L., Computer Emulation of Human Mental Processes of Neural Network Simulators to Problems in Well Log Interpretation, SPE 19619, 1989, October 8-11.

Xian, F.X.; Chork, C.Y.; Taggart, I.J; Mckay, D.M.; Barlett, R.M., A Genetic Approach to Prediction of Petrophysical Properties, Journal of Petroleum Geology, vol 17 (1), January 1994, pp. 71-88.

Aplicación de la Geostadistica en definicion de Esquemas Optimo de Exploracion de un Yacimiento Eoceno. Por I. Garcia y W. Poquioma , SVIP-058.

Acknowledgements

The authors would like to thank Xiomara Verenzuela and Fernando Chacartegui of Petróleos de Venezuela for providing the data that was used in this study.

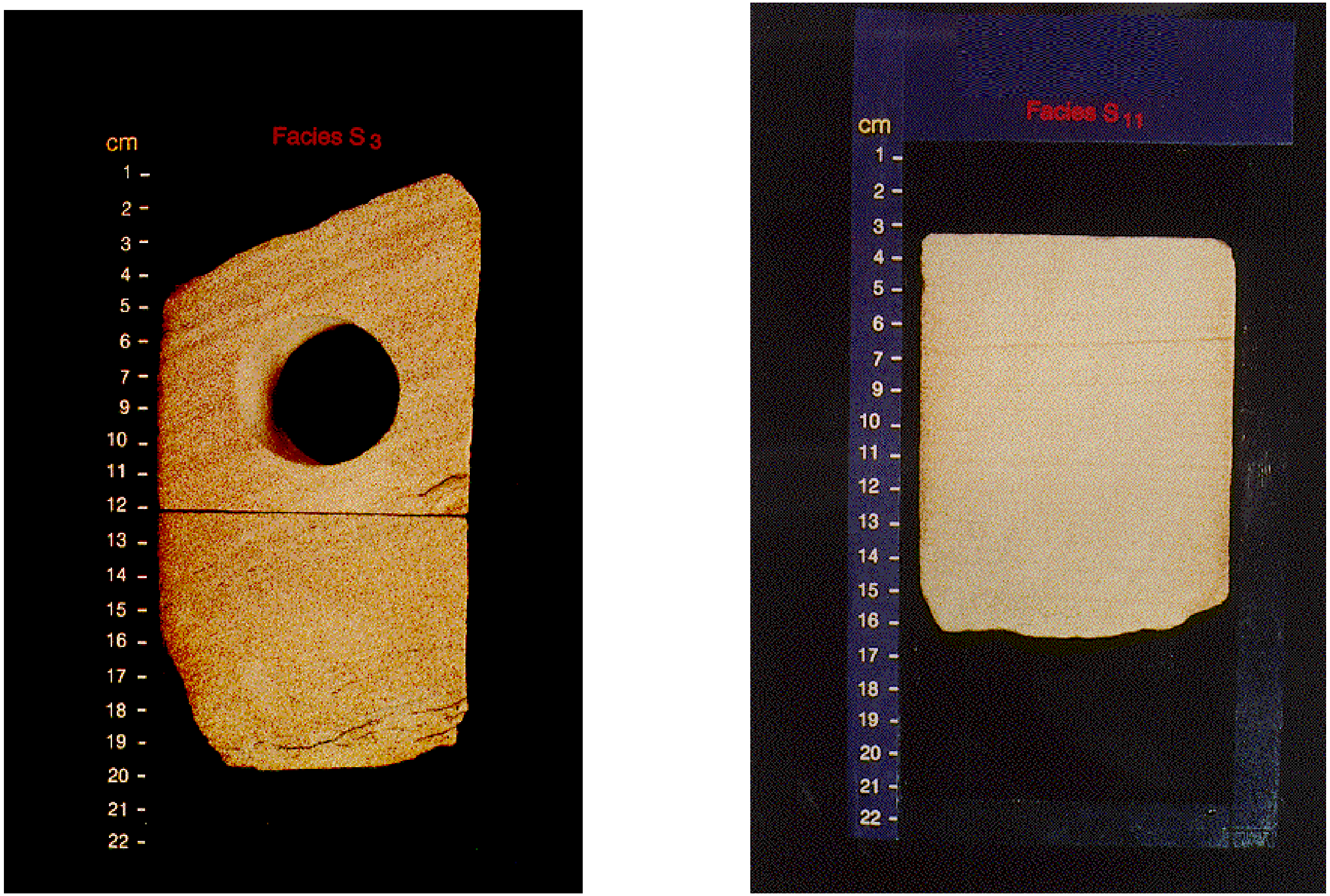

Fig. 1A Photographs of lithofacies S3 and S11 as described in Table 1 above.

Fig. 1B Photographs of lithofacies S2 and S31 as described in Table 1 above.

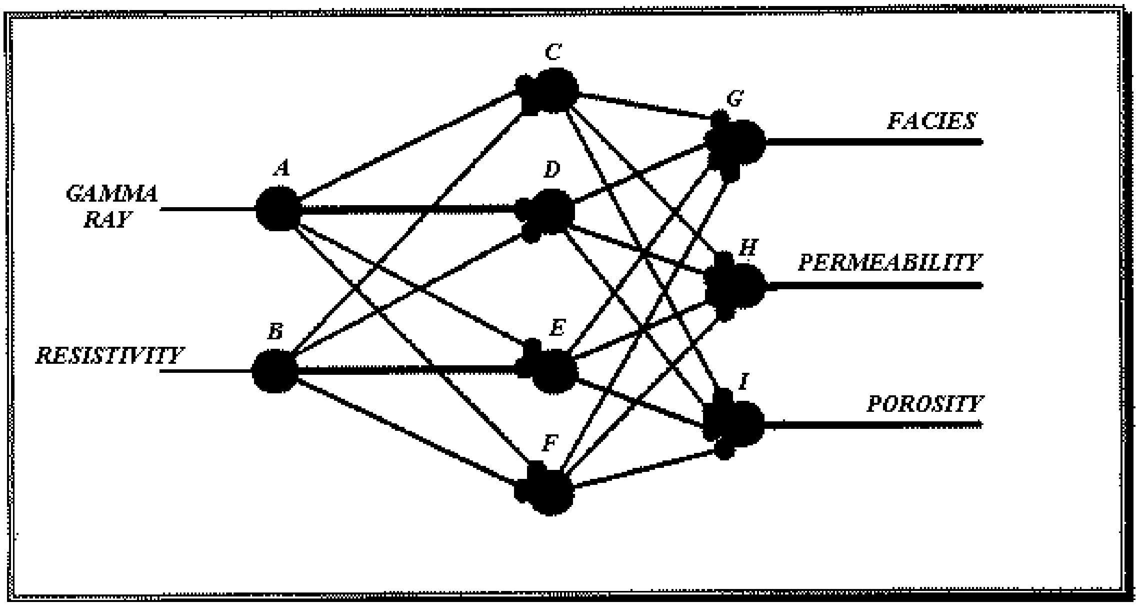

Fig. 2 shows a schematic of a typical neural network used in petrophysical evaluation. The number of nodes in the entry, hidden and output layers will vary depending on the application.

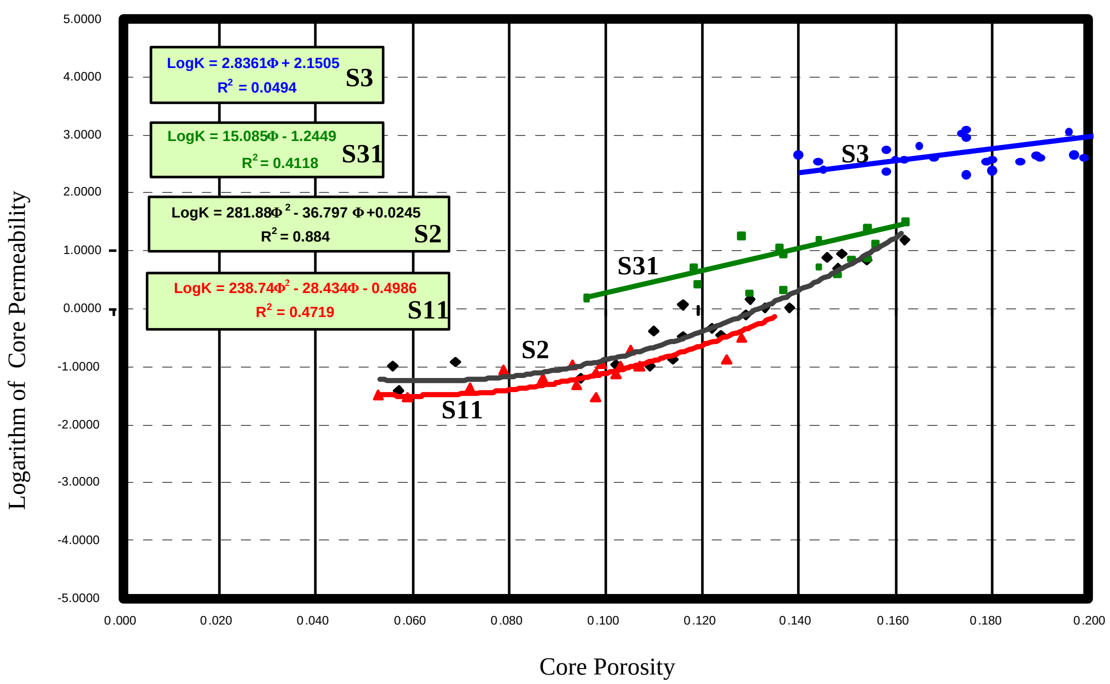

Fig. 3 Facies correlation for S3, S31, S2 and S11, in sand units C2 and C3

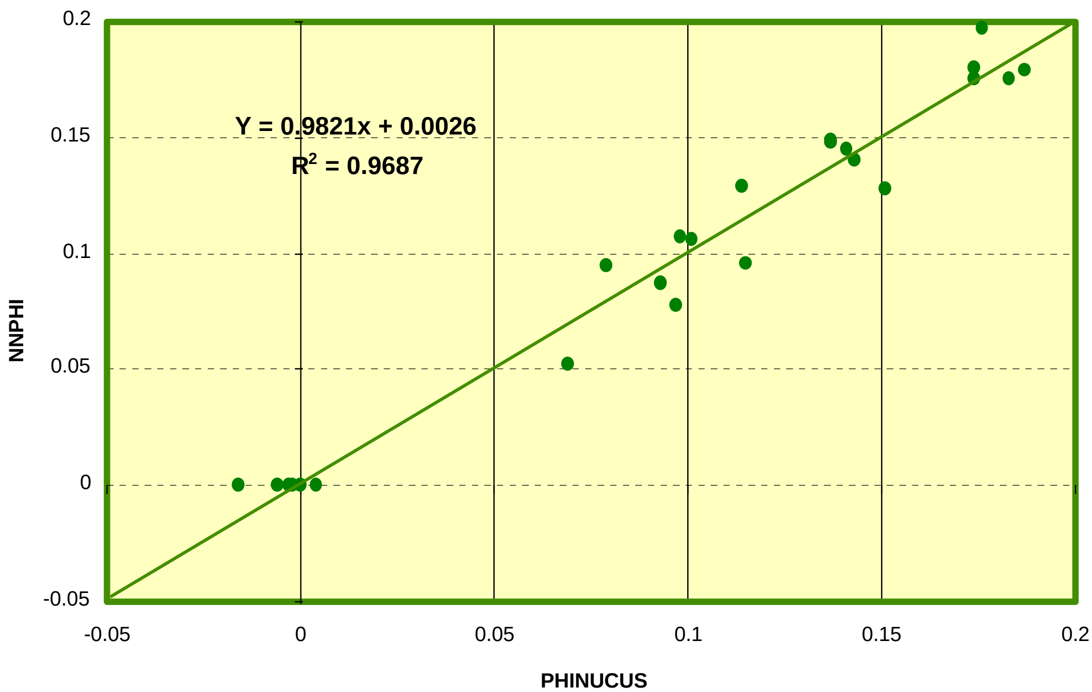

Fig. 5 shows the relationship between neural network porosity and core porosity

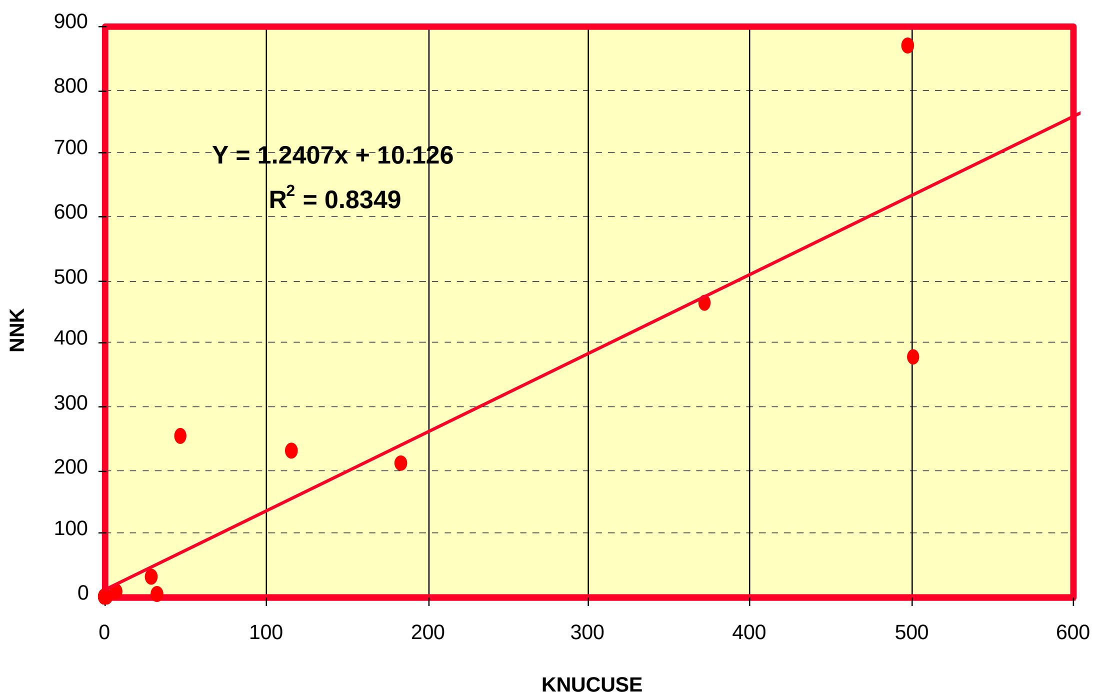

Fig. 6 shows the relationship between neural network permeability and core permeability

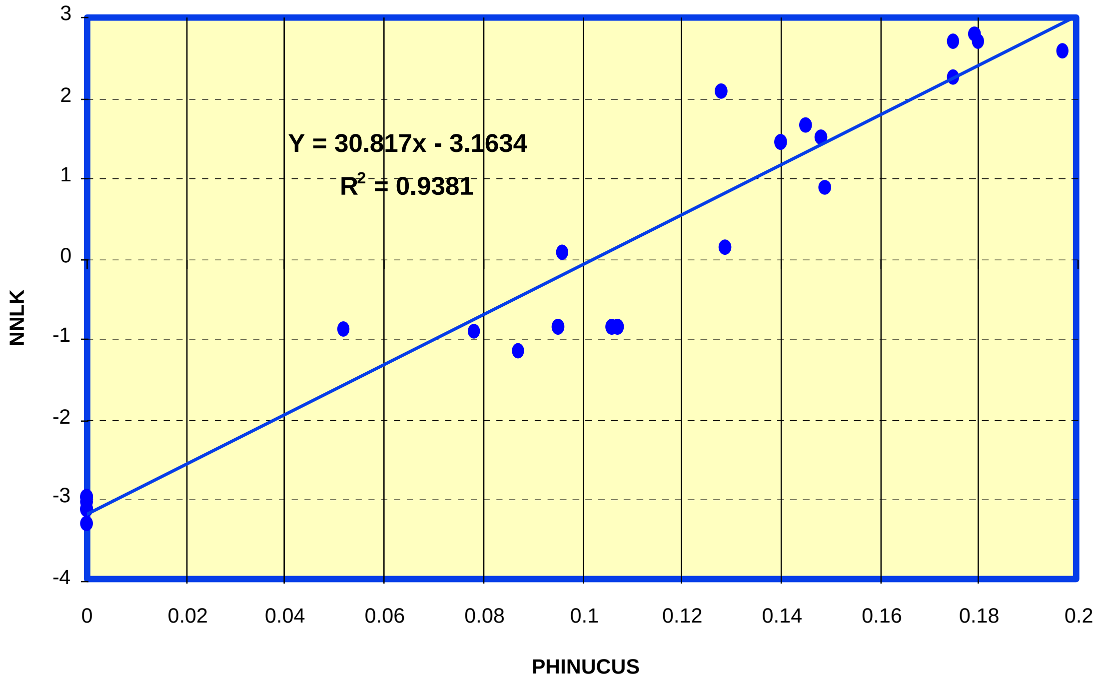

Fig. 7 shows the relationship between neural network permeability logarithm and core porosity